Molecular Medicine

Simvastatin and a Plant Galactolipid Protect Animals from Septic Shock by Regulating Oxylipin Mediator Dynamics through the MAPK-cPLA$_2$ Signaling Pathway

Maria Karmella Apaya,[1,2,3] Chih-Yu Lin,[2] Ching-Yi Chiou,[2] Chung-Chih Yang,[2,4] Chen-Yun Ting,[2] and Lie-Fen Shyur[1,2,4,5,6]

[1]Molecular and Biological Agricultural Sciences Program, Taiwan International Graduate Program, Academia Sinica, Taipei, Taiwan; [2]Agricultural Biotechnology Research Center, Academia Sinica, Taipei, Taiwan; [3]Graduate Institute of Biotechnology, National Chung Hsing University, Taichung, Taiwan; [4]Program for Cancer Biology and Drug Discovery, College of Medical Science and Technology, Taipei Medical University, Taipei, Taiwan; [5]Biotechnology Center, National Chung Hsing University, Taichung, Taiwan; [6]Graduate Institute of Pharmacognosy, Taipei Medical University, Taipei, Taiwan

Sepsis remains a major medical issue despite decades of research. Identification of important inflammatory cascades and key molecular mediators are crucial for developing intervention and prevention strategies. In this study, we conducted a comparative oxylipin metabolomics study to gain a comprehensive picture of lipid mediator dynamics during the initial hyperinflammatory phase of sepsis, and demonstrated, in parallel, the efficacy of simvastatin and plant galactolipid, 1,2-di-*O*-α-linolenoyl-3-*O*-β-galactopyranosyl-sn-glycerol (dLGG) in the homeostatic regulation of the oxylipin metabolome using a lipopolysaccharide (LPS)-induced sepsis C57BL/6J mouse model. LPS increased the systemic and organ levels of proinflammatory metabolites of linoleic acid including leukotoxin diols (9-,10-DHOME, 12-,13-DHOME) and octadecadienoic acids (9-HODE and 13-HODE) and arachidonic acid-derived prostanoid, PGE_2, and hydroxyeicosatetraenoic acids (8-, 12- and 15-HETE). Treatment with either compound decreased the levels of proinflammatory metabolites and elevated proresolution lipoxin A_4, 5(6)-EET, 11(12)-EET and 15-deoxy-PGJ_2. dLGG and simvastatin ameliorated the effects of LPS-induced mitogen-activated protein kinase (MAPK)-dependent activation of cPLA$_2$, cyclooxygenase-2, lipoxygenase, cytochrome P450 and/or epoxide hydrolase lowered systemic TNF-α and IL-6 levels and aminotransferase activities and decreased organ-specific infiltration of inflammatory leukocytes and macrophages, and septic shock-induced multiple organ damage. Furthermore, both dLGG and simvastatin increased the survival rates in the cecal ligation and puncture (CLP) sepsis model. This study provides new insights into the role of oxylipins in sepsis pathogenesis and highlights the potential of simvastatin and dLGG in sepsis therapy and prevention.

Online address: http://www.molmed.org
doi: 10.2119/molmed.2015.00082

INTRODUCTION

Sepsis syndrome encompasses a continuum of conditions ranging from acute systemic inflammation, sepsis, severe sepsis and septic shock following pathogen invasion to cytokine storm, multiorgan dysfunction and hypotension (1). Despite decades of research dedicated to understanding disease pathophysiology, early diagnostics, therapies and preventive strategies remain elusive. To date, clinical interventions include vaccination, broad-spectrum antibiotics, cytokine therapy and respiratory and metabolic support (2); however, mortality rates are still high at 30% for sepsis, 50% for severe sepsis and 80% for septic shock among patients (3). Identification of key molecular mediators other than the well-characterized cytokine players IL-1β and TNF-α orchestrating these tightly regulated signaling cascades may advance our basic understanding of sepsis syndrome.

Endogenous lipid mediators, particularly oxylipins derived from the oxidation of phospholipase-released polyunsaturated fatty acids (PUFAs), including linoleic acid (LA), α-linolenic acid (ALA), arachidonic acid (AA), docosahexaenoic acid (DHA) and eicosapentaenoic acid (EPA), through the action of cycloxygenases (COX), lipoxygenases (LOX) or cytochrome 450 (CYP450), are involved in the intricate inflammatory and resolution signaling systems in several disease conditions (4). Research on eicosanoids, resolvins and protectins has provided

Address correspondence to *Lie-Fen Shyur, Agricultural Biotechnology Research Center, Academia Sinica, No. 128, Sec. 2, Academia Road, Nankang, Taipei 115, Taiwan. Phone: +886-2-26515028; Fax: +886-2-26515028; E-mail: lfshyur@ccvax.sinica.edu.tw.*
Submitted April 7, 2015; Accepted for publication December 12, 2015; Published Online (www.molmed.org) December 14, 2015.

insights into the role of these molecular classes in active inflammatory processes, suggesting that they are important for the maintenance of normal organ function and cellular signaling (5–7). As there is a very fine line separating hyperinflammatory and immunosuppressive responses, we propose that examination of specific ratios, flux and interaction among different endogenous oxylipin classes may untangle the roles of lipid mediator signaling in sepsis. This approach may help us understand inflammatory conditions such as sepsis (8) and develop effective therapeutic and diagnostic tools.

One agent that has shown potential in sepsis therapy is simvastatin, a lipid-lowering drug targeting 3-hydroxy-3-methylglytaryl coenzyme A (HMG-CoA) reductase, which also exhibits pleiotropic antiinflammatory, antiplatelet and vasodilatory activities (9–12). Results of a randomized, double-blind, placebo-controlled clinical trial associated simvastatin administration with lower levels of inflammatory cytokines in patients with acute bacterial infections while another study suggested that prior statin therapy may have a role in the primary prevention and management of severe sepsis syndrome (13–15). Nutritional substrates, including omega-3 PUFA-enriched fish oils and plant sources that contain galactolipids (such as green vegetables and soybeans) have also been shown to modulate pathways involved in the release of inflammatory cytokines or a few types of eicosanoids (16,17). However, their effects on the systemic and organ-specific levels of endogenous oxylipin metabolites in the context of sepsis have not been explored fully.

In this study, we investigated oxylipin dynamics in sepsis and, in parallel, revealed the mechanisms of action associated with the preventive or therapeutic effects of simvastatin and a plant galactolipid, 1,2-di-*O*-α-linolenoyl-3-*O*-β-galactopyranosyl-*sn*-glycerol (dLGG), isolated from a medicinal plant *Crassocephalum rabens* (Asteraceae) in our laboratory (18) (Figures 1A, B). We explored the pathways related to the

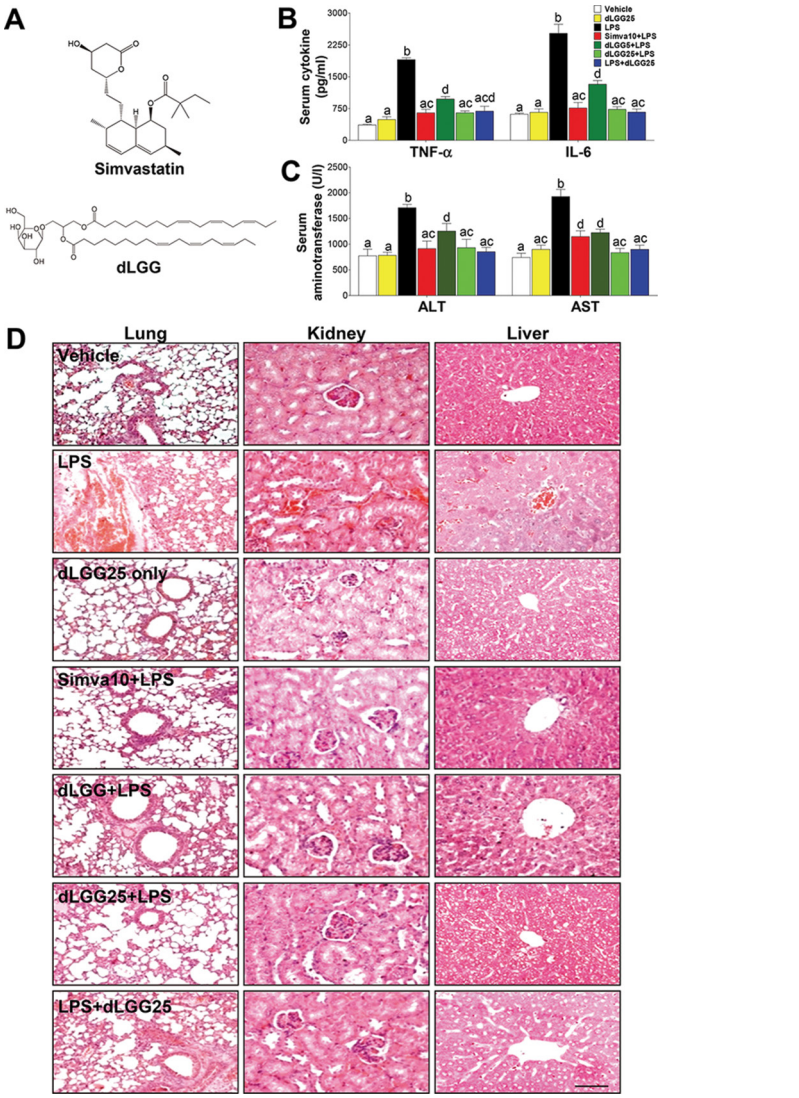

Figure 1. Organ architecture serum inflammatory cytokine levels, and aminotransferase activities in septic mice treated with simvastatin or dLGG. (A) Chemical structure of simvastatin, a cholesterol-lowering drug and inhibitor of HMG CoA reductase, and 1,2-di-*O*-α-linolenoyl-3-*O*-β-galactopyranosyl-*sn*-glycerol (dLGG), a plant galactolipid isolated from *Crassocephalum rabens*. (B) Comparison of levels of proinflammatory cytokines, TNF-α and IL-6, in sera of mice treated with DMSO (vehicle control), 25 mg/kg dLGG (dLGG25 only), 5 mg/kg LPS (LPS) only, 10 mg/kg simvastatin (Simva10 + LPS) and low-dose (dLGG5 + LPS) and high-dose (dLGG25 + LPS) dLGG pretreatment and (LPS + dLGG25) posttreatment. Simvastatin and dLGG were administered 1 h prior to LPS in the pretreatment groups, and dLGG was administered 1 h after LPS in the posttreatment group ($N = 4$, $P < 0.05$, ANOVA, *post hoc* LSD; values with different letters are significantly different). (C) Levels of aminotransferases, aspartate aminotransferase (AST) and alanine aminotransferase (ALT), from the sera of mice from the vehicle control, and LPS and simvastatin and dLGG treatment groups ($N = 4$, $P < 0.05$, ANOVA, *post hoc* LSD; values with different letters are significantly different). (D) Pathological examination of organ morphology and architecture among the treatment groups by H&E staining. Integrity of portal veins in the liver, alveolar sacs in the lungs and renal glomeruli, as well as the presence of inflammatory cells in all the treatment groups were compared with the vehicle control treatment (scale bar = 100 μmol/L).

homeostatic regulation of the oxylipin metabolome using an UPLC-MS/MS–based comparative metabolomics approach in the serum and liver of endotoxin (LPS)-induced septic mice. We present the phenotypic oxylipin profiles and associated protein targets leading toward antiinflammation and proresolution in the early stages of sepsis. Working models of the mechanistic action of the clinical drug simvastatin and the antiinflammatory phytoagent dLGG against septic pathogenesis and damage in mice are proposed.

MATERIALS AND METHODS

Plant Materials and Isolation of dLGG

dLGG with >98% purity was isolated from whole *C. rabens* plant (voucher specimen CB001, Agricultural Biotechnology Research Center, Academia Sinica, Taipei, Taiwan) following protocols previously described (17).

Cell Lines and Culture Conditions

Murine macrophages RAW264.7 obtained from American Type Culture Collection (ATCC) were grown in Dulbecco's modified Eagle medium (DMEM) (Gibco/BRI) supplemented with 10% heat-inactivated fetal bovine serum, 100 U/mL penicillin and 100 μg/mL streptomycin in a 5% CO_2 incubator at 37°C humidified atmosphere.

Measurement of Proinflammatory Cytokines and Aminotransferases, and Lipoxygenase Enzymatic Activity Assays

Production of proinflammatory cytokines, TNF-α and IL-6 (R&D Systems), and activities of aspartate transaminase (AST) and alanine transaminase (ALT) (Randox Laboratories) in mouse serum were determined using enzyme-linked immunosorbent assay (ELISA) kits according to the manufacturer's instructions. 5-lipoxygenase activity was measured using a screening kit as per the manufacturer's instructions (Cayman Chemical).

Western Blot Analysis of MAPK Signaling-Related Proteins

One hundred μL of 2×10^5 RAW 246.7 cells/mL plated in 96-well plates overnight were treated with compound for 1 h and then incubated for 24 h with or without LPS. NO production in the presence of specific inhibitors known to inhibit MAPK proteins in RAW 264.7 cells was determined. Inhibitors TAK242 (120 nmol/L), IMD0354 (20 μmol/L), SB203580 (1 μmol/L), PD0325901 (2 μmol/L) and SP600125 (90 nmol/L) for TLR4, IKK, p38, MEK 1/2 and JNK, respectively, were used. The same treatments were applied for Western blot analyses.

Western Blot Analysis of Relevant Proteins from Liver Homogenates

Total cellular proteins and tissue homogenates were extracted using radioimmunoprecipitation assay (RIPA) buffer containing protease and phosphatase inhibitors. Mouse tissues (0.1 g) were homogenized using a mixer ball mill (MM301, Retsch) for 2 min, extracted by adding 0.4 mL RIPA lysis buffer and centrifuged at 15,115 × *g* for 30 min at 4°C. The supernatant was collected and total protein concentrations of samples were determined by using a DC protein assay kit (Bio-Rad). Proteins were separated by 10% SDS-PAGE and electrotransferred into PVDF membrane (Immobilon). The blots were incubated in blocking buffer (5% BSA in Tris-buffered saline) for 1 h then with specific antibody overnight at 4°C. After washing, blots were incubated in appropriate antibodies conjugated with horseradish peroxidase (HRP) for 3 h at room temperature. Immunoreactive bands were visualized using enhanced chemiluminescence reagents (GE Healthcare Life Sciences).

Animal Studies

All animal care and experimental procedures were approved by the Institutional Animal Care and Utilization Committee (IACUC) of Academia Sinica (Taipei, Taiwan) and reported in compliance with the Animal Research: Reporting In Vivo Experiments (ARRIVE) guidelines for reporting experiments involving animals. Female C57BL/6J mice (4 wks old) from the National Laboratory Animal Center in Taipei, Taiwan were used in this study. Mice were acclimatized for 1 wk, supplied with water, fed *ad libitum* and kept in a 12 h light/dark cycle at 22 ± 2°C. Two animal models were utilized in this study to mimic the initial hyperinflammatory phase (LPS-induced endotoxemia) and the compensatory immunosuppressive phase (CLP) of sepsis in mice. For the endotoxemia model, mice were randomly separated into groups and pretreated orally with vehicle, dLGG only (25 mg/kg body weight; dLGG25), simvastatin (10 mg/kg body weight; Simva10) and dLGG (5 and 25 mg/kg body weight; dLGG5 and dLGG25) before challenge with LPS (5 mg/kg body weight; LPS) for 24 h. To study the therapeutic effect of dLGG, one group was treated with 25mg/kg dLGG 1 h post-LPS challenge (LPS + dLGG25). For the CLP model, mid-grade sepsis was induced as described previously (19). Briefly, mice were anesthetized by intraperitoneal injection of a commercial mixture of zolazepam, xylazine and atropine (Virbac Animal Health) prior to making a 3- to 5-mm midline laparotomy. The cecum was then exposed and ligated (3-0 silk suture) distal to the ileocecal valve to prevent intestinal obstruction and punctured twice with an 18G needle. The punctured cecum was squeezed gently to expel a small amount of fecal matter for induction of polymicrobial sepsis before returning it to the abdomen and closing the peritoneal wall and skin incisions. One mL of saline was administered subcutaneously for fluid resuscitation. The same surgical procedure, except for the CLP steps, was carried out on sham-operated animals that served as controls. The preventive effects of dLGG and simvastatin on survival were assessed by treatment with dLGG25 and Simva10 for 3 d prior to CLP, while therapeutic effects were assessed by treatment with dLGG25 post-CLP operation. Mortality rate of tested animals was recorded for 10 d.

Histopathological Examination

After retro-orbital collection of blood, mice were killed by cervical dislocation and organs (kidneys, lungs and liver) were removed. One set of organs was flash frozen using liquid N_2 and another set was fixed with 10% paraformaldehyde. Sera were collected by centrifugation of whole blood at 15,115 × *g* for 30 min at 4°C. Paraffin-embedded samples were sectioned (6 μm for liver tissues and 4 μm for kidney and lung tissues) and stained with hematoxylin and eosin (H&E). Paraffin-embedded organ sections were heat-immobilized and deparaffinized using xylene, and rehydrated in a graded series of ethanol with final washing using distilled water. Immunohistochemistry was performed by using a commercial antigen retrieval buffer, Target Retrieval Solution (DakoCytomation), and a Decloaking Chamber (Biocare Medical) before incubating the samples in primary antibody overnight at 4°C. After subsequent washing, tissues were incubated using appropriate fluorescent secondary antibodies. Protein expressions were visualized by immunofluorescent imaging using AxioVision software (Carl Zeiss MicroImaging).

Preparation of Oxylipin Samples from Serum and Liver Tissues

Mice serum and liver samples were collected immediately and flash frozen with liquid N_2 and stored at –80°C. Modified Folch extraction solvent, $CHCl_3$:MeOH (2:1) + 0.1 mol/L DHT and 0.01 mol/L TPP, was added to serum or liver homogenate. Ten mL of internal standard solution was added. The solution was kept in ice for 20 min before centrifugation at 15,115 × *g* for 10 min at 4°C. The organic layer was collected in a new microcentrifuge tube and recentrifuged twice to remove debris (6). Four biological repeats and five technical repeats for each group were subjected to LC-MS/MS analysis.

Chemical Profiling of Mouse Oxylipin Markers

Two different types of compounds were used as internal standards. Type I internal standards were added to samples before extraction to account for the extraction efficiency of prostaglandins, diols, epoxides and other oxylipins. Type II internal standard, CUDA, was added to account for changes in volume and instrument variability. Relative retention times and fragmentation signatures of internal standards were used to optimize conditions and identify corresponding metabolite peaks in the samples. Corresponding Type I internal standards, based on the chemical structure/parent molecule, were used for relative quantification of metabolites. Each biological sample was spiked with internal standard solution containing 0.1 ppm each of isotopic standards PGE_2-d4, 5-HETE-d8, DHA-d5, 6-keto-PGF_{1a}-d4, EPA-d5, 9-HODE-d4, 20-HETE-d6 and CUDA.

Analysis and Quantitative Profiling of Oxylipin Metabolome by Liquid Chromatography–Electrospray Ionization–Tandem Mass Spectrometry (LC-ESI-MS/MS)

The system used for analysis was an ultraperformance liquid chromatography (UPLC) system (ACQUITY UPLC, Waters) coupled with a TSQ Quantum Access Max (Thermo Fisher Scientific) triple quadrupole mass spectrometer. The sample was separated with an ACQUITY UPLC HSS T3 column (particle size 1.8 μm, 2.1 × 100 mm, Waters) at 400 μL/min flow rate using 25 min gradient for analysis. Mobile phase A consisted of 0.1% NH_4OH in water and mobile phase B consisted of 0.1% NH_4OH in MeOH. The instrument was operated in negative multiple reaction monitoring (MRM) mode. Precursor and most abundant fragment ions for quantification of each analyte were obtained by scanning individual analyte standards separately in MS full-scan mode and product ion scan mode. The source parameters and collision energy of each analyte were optimized by direct infusion. The MS operating conditions were optimized as follows: spray voltage, 3.2 kV; vaporizer temperature, 300°C; ion transfer capillary temperature, 270°C; sheath gas (nitrogen), 40 Arb; auxiliary gas (nitrogen), 5 Arb; collision gas (argon) pressure, 1 mTorr. Matrix effect was compensated for by adding 10 μL of all serum samples to the standard solution and checking shifts in retention time and peak intensities.

Data Processing

The chromatogram acquisition, detection of mass spectral peaks and waveform processing were performed using ThermoXcalibur 2.1 SP1 software (Thermo Scientific). The calibration curve and quantification were performed using LCQuan 2.6.1 software (Thermo Scientific). The peak area of each quantified ion was calculated and normalized against the peak area of the corresponding internal standards. Coefficient of variation (CV), <15% for five technical replicates and <30% for each biological sample, respectively, was used to assess deviation and data inclusion.

Statistical Analysis

SPSS v16.0 was used for data analysis. All data are expressed as mean ± SEM. Differences were compared by analysis of variance (ANOVA), followed by *post hoc* least significant difference (LSD) test. Different letter superscripts indicate significant difference within treatments with $P < 0.05$. Multivariate data analysis was carried out using SIMCA-*P* 11.0 software (Umetrics). Principal component analysis (PCA) and partial least squares-discriminant analysis (PLS-DA) were used for clustering and analyzing the metabolic alterations within different sample groups and treatments.

Materials

Oxylipin standards (47 compounds) were purchased from Cayman Chemical. All other chemicals and solvents were of reagent or high-pressure liquid chromatography (HPLC) grade. Butylated hydroxytoluene (BHT) and triphenylphosphonium (TPP) used as antioxidant additives for oxylipin extraction were purchased from Sigma. Linoleic acid metabolite standards were (±)9-hydroxy-10*E*,12*Z*-octadecadienoic acid (9-HODE); 13-HODE;

(±)12(13)-epoxy-9*Z*-octadecenoic acid (12,13-EpOME); (±)9(10)-EpOME; (12*Z*)-9,10-dihydroxy-12*Z*-octadecenoic acid (9,10-DiHOME); 12,13-DiHOME; 13-keto-9*Z*,11*E*-octadecadienoic acid (13-oxo-ODE); 9-oxo-ODE; 9,10,13-tri-hydroxyoctadecenoic acid (9,10,13-TriHOME); and 9,12,13-TriHOME. Arachidonic acid metabolite standards were 9S,11R,15S-trihydroxy-5*Z*,13*E*-prostadienoic acid ($PGF_{2\alpha}$); 11-oxo-5*Z*,9,12*E*,14*E*-prostatetraenoic acid (15-deoxy-PGJ_2); 6-oxo-9S,11R,15S-trihydroxy-13*E*-prostenoic acid (6-keto-$PGF_{1\alpha}$); thromboxane B_2 (TXB_2); prostaglandin D_2 (PGD_2); PGE_2; 5-hydroxyeicosatetraenoic acid (5-HETE); 8-HETE; 9-HETE; 11-HETE; 12-HETE; 15-HETE; 20-HETE; 15-oxo-eicosatetraenoic acid (15 oxo-ETE); 5 oxo-ETE; 14,15-ep oxy-5*Z*,8*Z*,11*Z*-eicosatrienoic acid (14(15)-EET); 11(12)-EET; 8, 9-EET; 5(6)-EET; 14,15-dihydroxy-5*Z*,8*Z*,11*Z*-eicosatrienoic acid (14,15-DHET); 11,12-DHET; 8,9-DHET; 5,6-DHET; 11,12,15-THET; leukotriene A_4 (LTA_4); LTB_4; 5*S*,6R,15S-trihydroxy-7*E*,9*E*,11*Z*,13*E*-eicosatetraenoic acid (LXA_4); LXB_4; THF diols–9,12-oxy-10,13-dihydroxy-octadecanoic acid and 10,13-oxy-9,12-dihydroxyoctadecanoic acid. 4*Z*,7*Z*,10*Z*,13*Z*,16*Z*,19*Z*-docosahexaenoic acid (DHA) and 5*Z*,8*Z*,11*Z*,14*Z*,17*Z*-eicosapentaenoic acid (EPA) metabolites included 7*S*,8R,17*S*-trihydroxy-4*Z*, 9*E*, 11*E*, 13*Z*, 15*E*, 19*Z*-decosahexaenoic acid (resolvin D_1); (±)17-hydroxy-4*Z*, 7*Z*, 10*Z*, 13*Z*, 15*E*, 19*Z*-docosahexaenoic acid (17-HDoHE); 10-17-DiHDoHE; (±)15-hydroxy-5*Z*, 8*Z*, 11*Z*, 13*E*, 17*Z*-eicosapentaenoic acid (15-HEPE); and 7R,14*S*-dihydroxy-4*Z*, 8*E*, 10*E*, 12*Z*, 16*Z*, 19*Z*-docosahexaenoic acid (7[*S*)]-Maresin 1). Type I internal standards (7) included 6-keto-$PGF_{1\alpha}$-d4, PGE_2-d4, 20-HETE-d6, 9-(S)-HODE-d4, 5-HETE-d8, 11(12)-EET-d8 and a non-endogenous monounsaturated fatty acid, 10,11-dihydroxynondecanoic acid (10,11-DHN). The type II internal standard used was 1-cyclohexyl-dodecanoic acid urea (CUDA). Antibodies used were as follows: MEK 1/2, phospho-MEK 1/2, $cPLA_2$, phospho-$cPLA_2$, p38, phospho-p38, IKK-α, phospho-IKK, phospho-JNK, phospho-ERK 1/2 (Cell Signaling); sEH, PPAR-γ, CYP4A (Abcam); COX-2 (Cayman); actin (Millipore); HIF-1α, JNK 1/2, ERK 1 (Santa Cruz); and COX-2 and F4/80 (Abnova). TAK242, IMD0354, SB203580, PD0325901 and SP600125 were purchased from Selleck Chemicals.

All supplementary materials are available online at www.molmed.org.

RESULTS

Simvastatin and dLGG Inhibit Secretion of Proinflammatory Cytokines and Aminotransferase Activities in Septic Mice

An endotoxin (LPS)-induced septic mouse model was used to study the preventive or therapeutic effects of simvastatin and dLGG against acute inflammation and septic shock *in vivo*. Pretreatment groups dLGG5 + LPS, dLGG25 + LPS, and Simva10 + LPS, and posttreatment groups LPS + dLGG25 or dLGG alone (dLGG25) were compared with vehicle control and LPS groups. We observed that LPS induced an approximate five-fold increase in the serum levels of TNF-α and IL-6. Conversely, treatment with Simva10 + LPS, dLGG25 + LPS and LPS + dLGG25 lowered the serum levels of TNF-α and IL-6 by four-fold and two- to 3.3-fold (Figure 1B). In the dLGG25 group, both cytokines were maintained at basal levels that were similar to the vehicle control. Serum enzymatic activities of hepatocyte-released aspartate transaminase (AST) and alanine transaminase (ALT) were increased in the LPS group compared with the vehicle control group by three-fold and 2.5-fold (Figure 1C), respectively, indicating serious hepatic damage associated with sepsis (20). dLGG pretreatment dose-dependently reduced serum AST levels by 1.5- to two-fold relative to the LPS-treated group, while ALT levels in the dLGG and simvastatin pretreatment groups were maintained at levels similar to the vehicle control. The dLGG treatment and the vehicle control groups had similar serum AST and ALT levels, suggesting that dLGG caused no side effects in test animals.

Simvastin and dLGG Attenuate Organ Damage Induced by LPS in Mice

The protective effects of simvastatin or dLGG treatment on endotoxin-induced multiple organ damage, a major pathophysiological characteristic of sepsis (21) were evaluated. In this study, LPS-induced septic shock in C57BL/6J mice resulted in phenotypic organ damage in the liver, lungs and kidneys, visualized by H&E staining (Figure 1D). Loss of sinusoidal epithelial integrity and infiltration of red blood cells into the hepatic central portal veins, destruction of glomerular structures and the presence of necrotic cells and erythrocytes in the kidneys, and acute lung distress (ALD) characterized by damage to alveolar sacs and arteries were observed following LPS challenge. This multiple organ damage was reversed or attenuated by treatment with either simvastatin or dLGG. Simvastatin- and dLGG-treated groups had similar tissue architecture to those of the vehicle control. Healthy mice treated with dLGG only also showed normal tissue architecture, indicating that dLGG administration alone had no harmful effects on organs.

Simvastin and dLGG Attenuate CLP-Induced Multiple Organ Damage and Lethality in Mice

To further examine the effect of compound treatment on different stages of sepsis progression, a mid-grade form of the CLP-induced sepsis mouse model was utilized. Multiple organ damage in mice was assessed at 24 h after CLP-induced sepsis by H&E staining of the liver, lungs and kidneys (Supplementary Figure S1A). Evident destruction of organ architecture was observed in the CLP-operated mice, for example, pulmonitis, loss of sinusoidal cells or erythrocyte influx/hemorrhage in the liver,

and significant glomerular congestion and tubular epithelial atrophy in kidney tissues, whereas the dLGG- and simvastatin-treated mice showed similar organ structural patterns as the sham control group. Serum enzymatic activities of AST and ALT, systemic indicators of hepatic damage, were decreased by treatment with either compound (Supplementary Figure S1B).

CLP-induced sepsis resulted in a 40% survival rate after 3 d and subsequently, a 100% mortality rate within 10 d after CLP operation. Pretreatment with either dLGG (25 mg/kg) or simvastatin (10 mg/kg) for 3 d prior to CLP resulted in 70% and 50% survival rates, respectively, after 3 d (N = 10). After the 10 d observation period, 70% of the pre- and post-dLGG-treated mice survived, while only 20% survived in the simvastatin-treated group (Supplementary Figure S1C), demonstrating that the novel preventive efficacy of dLGG is superior to that of simvastatin against CLP-induced lethality in septic mice.

Simvastatin and dLGG Modulate Organ-Specific Infiltration of Inflammatory Leukocytes, COX-2 Overexpression in the Liver, PPAR-γ Overexpression in the Lungs and Hypoxia in the Kidneys

We used immunofluorescence staining to investigate the organ-specific protective effects of simvastatin and dLGG. We chose to colocalize several organ markers with infiltrating or activated resident immune cells as an indicator of the severity of organ damage. Hepatic activation of COX-2 can induce macrophage activation and recruitment, which are crucial in systemic cytokine and lipid mediator production at the onset of sepsis (22). A three-fold increase in infiltrating F4/80$^+$ macrophages and activated Kupffer cells was seen in the LPS group compared with the vehicle control group (Figure 2A). In the groups treated with dLGG or simvastatin F4/80$^+$-infiltration was prevented or reversed to the basal level by 24 h after LPS administration. Endotoxin-induced hepatic COX-2 overexpression, colocalized with F4/80$^+$ infiltrated cells, was attenuated three-fold by simvastatin and two-fold by dLGG. We also measured HIF-1α protein expression and the infiltrating F4/80$^+$ macrophage population in the kidney as renal hypoxia and macrophage recruitment in the kidney glomeruli indicates an advancing degree of systemic inflammation (23). HIF-1α expression colocalized with infiltrated macrophages in the LPS group, and was two-fold higher than that of the vehicle control (Figure 2B). Simvastatin or dLGG treatment attenuated HIF-1α expression and macrophage infiltration to levels comparable to the vehicle basal values.

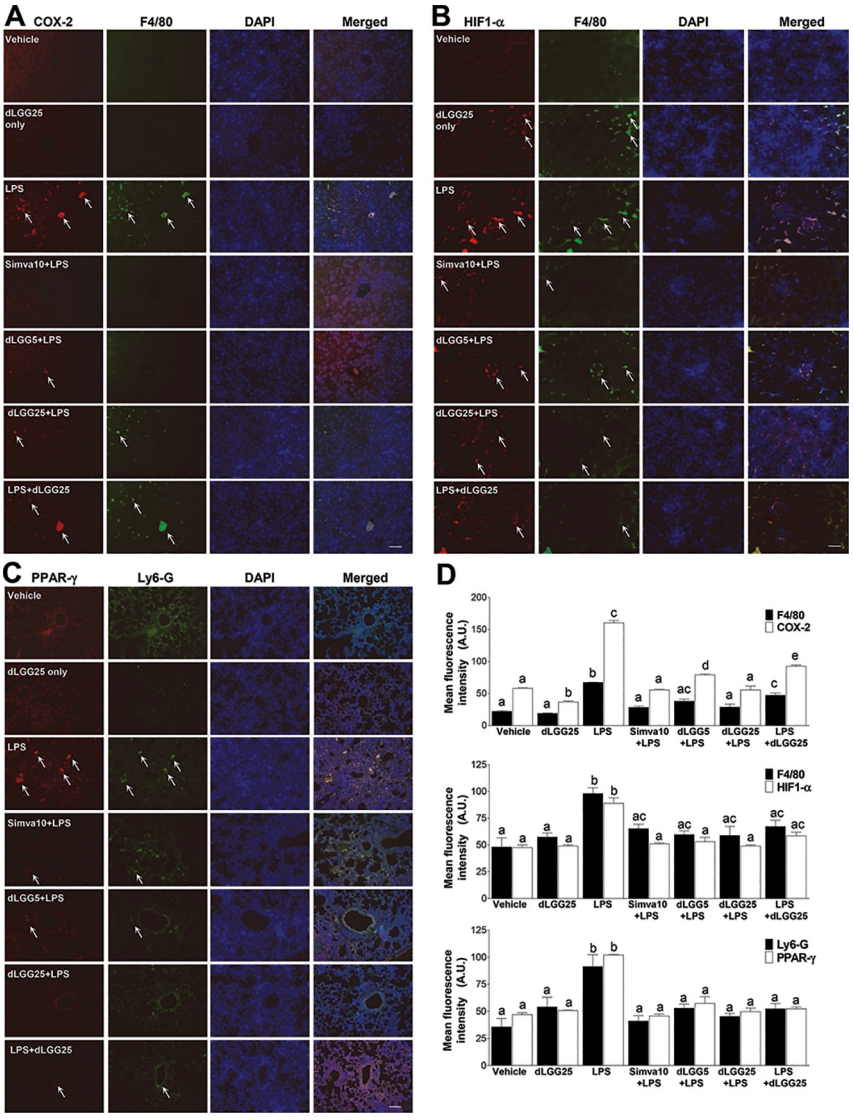

Figure 2. Immunofluorescence staining of inflammatory markers in the liver, lungs and kidneys. Representative immunofluorescence staining images of (A) hepatic COX-2 expression and F4/80$^+$ cell population in the sinusoids of the liver tissue, (B) HIF-1α expression and F4/80$^+$ cell population in the renal glomeruli of the kidney tissue, and (C) PPAR-γ expression and Ly6G$^+$ cell population in the lung alveoli (scale bars = 50 μmol/L). (D) Graphical representation of mean fluorescence intensities for proteins detected in each image were normalized against background intensities of the vehicle control group, expressed as arbitrary fluorescence units (A.U.) (N = 4, P < 0.05, ANOVA, *post hoc* LSD; values with different letters are significantly different).

In the lungs, we measured the level of PPAR-γ expression, a ligand-activated transcription factor constitutively expressed in the lung epithelium, which is also prominently expressed in activated leukocytes, for example, neutrophils and macrophages, and is upregulated by proinflammatory cytokines (24). Quantified fluorescence images (Figure 2D) showed that LPS treatment increased PPAR-γ expression in the lung tissues by 2.5-fold compared with the vehicle control group, which was partly due to the influx of Ly6-G^+ neutrophils. In the dLGG-alone, Simva10 + LPS, dLGG25 + LPS, and LPS + dLGG25 treatment groups, PPAR-γ expression was detected at basal levels after treatment for 24 h (Figure 2C). The increased presence of $Ly6G^+$ granulocytic neutrophils in the LPS group confirmed an active inflammatory process, which was attenuated by simvastatin and dLGG in a dose-dependent manner. In the CLP-induced sepsis mouse model, we have observed profound Ly6-G^+ neutrophil infiltration but less PPAR-γ expression in the lung tissues of the CLP group than the sham control (Supplementary Figure S2). Pre-dLGG, post-dLGG and pre-Simva10 treatment significantly inhibited CLP-induced Ly6-G^+ neutrophil infiltration along with a notable increase of PPAR-γ expression in mouse lung tissues (Supplementary Figure S2). Together with the maintenance of normal organ tissue architecture in the treatment groups (Figure 1D and Supplementary Figure S1), this suggests an active ongoing resolution of inflammation in septic mice. These results provide strong evidence that treatment with either simvastatin or dLGG can prevent multiple organ damage in sepsis.

Simvastatin and dLGG Modulate Systemic and Organ-Specific Release of Oxidized Lipid Mediators

Next, our study investigated the endogenous oxylipin metabolome in septic mice and whether the animals treated with either simvastatin or dLGG had an altered oxylipin balance toward homeostasis. We used a targeted metabolomics approach utilizing UPLC-MS/MS in multiple reaction monitoring (MRM) mode to examine the flux of 47 oxylipin species representative of AA, ALA, LA, EPA and DHA metabolites, within multiple catalytic pathways mediated by COX-2, LOX, CYP450,and sEH. We assessed the pro- and antiinflammatory and proresolution contribution of these species to local (liver) and systemic (serum) pathological phenotypes in sepsis. After normalization and quantification using isotopic standards, relative levels of specific oxylipins derived from these enzymatic pathways showed that simvastatin and dLGG treatments attenuated the increase in total systemic serum and liver oxylipin mediators caused by LPS treatment in animals (Figures 3A, B). Specific oxylipin concentrations after the different treatments are shown in Supplementary Tables 1 and 2. The oxylipin metabolome profile clustering (score and loading plots), and heatmap comparisons for levels of oxylipins are shown in Figures 3C and D. In the serum (Figure 3C), 8-HETE, 12-HETE, 15-HETE, TXB_2 and LXA_4 produced from the oxidation of AA by 8-, 12- and 15-LOX and COX enzymes stood out as outliers in the loading scatter plot and are the main discriminatory metabolites among the tested animals. 9,12,13-TriHOME, 9,10-DiHOME, 12,13-DiHOME, 12(13)-EpOME, 13-HODE and 9-HODE were also identified as important clustering components. Heatmap clustering demonstrated that, overall, the post-dLGG25 treatment group had an oxylipin profile that most closely resembled that of the vehicle control. The LA metabolites derived from LOX, that is, 9-HODE and 13-HODE; CYP450 epoxides, that is, 9(10)-EpOME and 12(13)-EpOME; and sEH metabolites, that is, 9,10-DiHOME, 12,13-DiHOME, 9,12,13-TriHOME and 9-oxo-ODE were significantly increased in the LPS group relative to all of the treatment groups including the vehicle control. Levels of AA metabolites 8-, 12-, 15-HETE, and 15-oxo-ETE in all the treatment groups were not significantly different from the vehicle whereas a two- to four-fold increase was observed in the LPS group (Figure 4A and Supplementary Table 1).

We also measured the oxylipin mediator levels in the liver, as this organ is a major site of lipid metabolism (Figure 3D). The score plot for the liver also shows clearly defined clustering patterns among the groups. 9(10)-EpOME, 12,13-DiHOME, 8-HETE and Lipoxin A_4 (LXA_4) were identified as outliers in the corresponding loading scatter plot. As with the systemic oxylipin profiles in the liver tissues, LA metabolites, 9- and 13-HODE, 12(13)-EpOME, 9,10- and 12,13-DiHOME; 19,12-13-TriHOME were three- to ten-fold higher in the LPS group compared with the other groups, which were all at similar levels to the vehicle control. Among the AA metabolites, 5-oxo-ETE, PGE_2 and $PGF_{2\alpha}$, and 19-HETE were most significantly elevated in the LPS group. LXA_4 was not detected in the liver of vehicle-, LPS- and dLGG-only-treated mice whereas this metabolite was detected in high amounts in the liver of the Simva10 + LPS, dLGG25 + LPS, and LPS + dLGG25 treatment groups (Figure 4B).

Figure 4C summarizes the significant increases in the serum levels of LXA_4 (three-fold) and 5(6)-EET (five-fold) in simvastatin, and 11(12)-EET (seven-fold) in the dLGG25 pretreatment group, thus demonstrating the differential effect of the two compounds on the oxylipin profile against LPS-induced sepsis in mice. Natural PPAR-γ ligand, 15-deoxy-PGJ_2, was increased, and PGE_2 was decreased by both simvastatin and high-dose dLGG treatment. DHA and EPA metabolites, that is, resolvin D1, 17-HDoHE, 10,17-DiHDoHE and 15-HEPE, however, were not detected in quantifiable amounts in the serum of any of the treatment groups. Interestingly, these metabolites were detected in appreciable amounts in the liver. In the LPS-treated group, DHA, EPA and their metabolites, resolvin D1 and 15-HEPE, were elevated two- to six-fold compared with the vehicle control. These levels were further

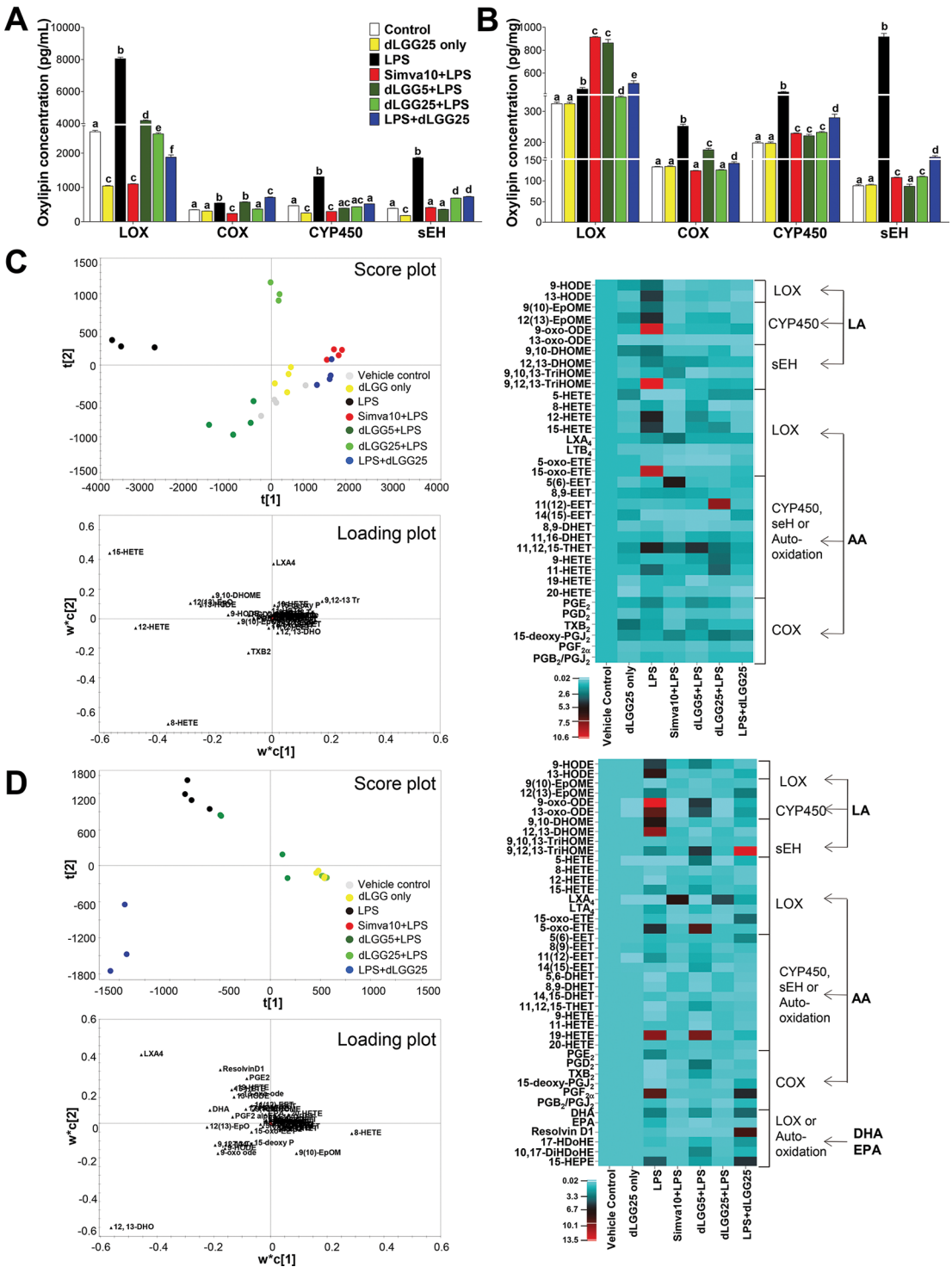

Figure 3. Comparative metabolomic profiling of systemic and organ-specific oxylipin mediators. (A) Total serum and (B) liver levels of oxylipin metabolites from the LOX, COX, CYP450 and sEH pathways. Concentrations are expressed in pg/mg and pg/mL in liver samples and serum samples, respectively. PLS-DA score plot and corresponding loadings plot derived from the quantified oxylipin levels in the (C) sera and (D) liver of the vehicle control, LPS only, and the different treatment groups. Corresponding heat maps are shown with oxylipin metabolites grouped according to precursor compounds (LA, AA, DHA and EPA) and the corresponding enzymes. DHA and EPA metabolites were not detected from the serum. (*N* = 4 per treatment group).

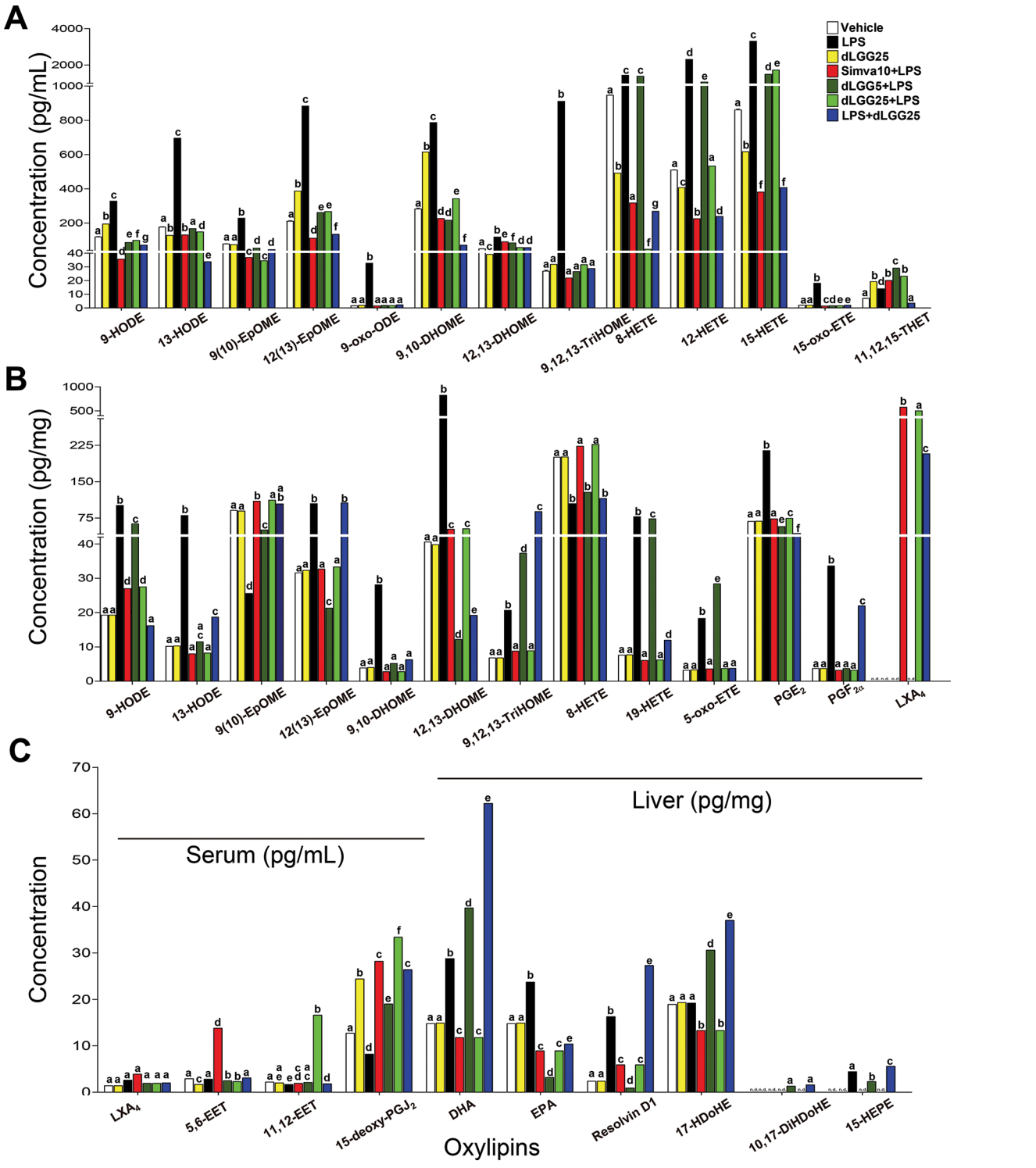

Figure 4. Quantitative comparison of individual oxylipin metabolite levels with significant contribution to the PLS-DA metabolite clustering in the sera and liver of septic mice. Concentrations are expressed in pg/mg and pg/mL for the liver sample and serum sample, respectively. Major contributors to (A) serum and (B) liver PLS-DA clustering were identified based on the loadings plot and quantified oxylipin levels. (C) Serum levels of proresolution and antiinflammatory oxylipins, LXA_4, 5(6)-EET, 11(12)-EET and 15-deoxy-PGJ_2, as well as hepatic levels of precursor DHA and EPA, corresponding proresolution metabolites resolvin D1, 17-HDoHE, 10,17-DiHDoHE, and 5-HEPE, increased by either dLGG or simvastatin treatment are shown ($N = 4$, $P < 0.05$, ANOVA, *post hoc* LSD; values with different letters are significantly different).

increased in the dLGG posttreatment group (Figure 4C). 15-HEPE, implicated in the active resolution process, was detected in the LPS, dLGG pre- and posttreatment groups.

Simvastatin and dLGG Lower Production of Proinflammatory Lipid Mediators via a MAPK-Dependent Pathway

Next, we investigated the underlying molecular mechanisms related to the observed phenotypic oxylipin profiles. We first determined that dLGG is a 5-LOX inhibitor using AA as the substrate, with an IC_{50} of 15 μmol/L; simvastatin at the measured concentrations up to 50 μmol/L showed only 15% inhibition on 5-LOX enzyme activity (Figure 5A). In our previous study, we demonstrated that dLGG is also a COX-2 enzyme inhibitor (18). These results indicate that dLGG directly alters oxylipin levels by competing with endogenous substrates of 5-LOX or COX-2 while simvastatin may do so through little direct enzyme interaction.

To validate the functional role(s) of specific signaling proteins, (MAPK, upstream TLR or the IKK proteins of the NF-κB cascade) involved in regulating the activation of downstream enzymes of $cPLA_2$, we treated LPS-stimulated RAW 264.7 macrophages with specific TLR4 (TAK242), IKKα (IMD0345), p38 (SB203580), MEK 1/2 (PD0325901) and JNK (SP600125) inhibitors. We chose these inhibitors to verify the correlation between activation of these upstream signaling events and the expression levels of $cPLA_2$—the major enzyme responsible for free fatty acid release via *sn*2 cleavage of membrane phospholipids, and its downstream enzymes, that is, 5-LOX and sEH, both of which are involved in oxylipin biosynthesis. The results show that treatment with any of the inhibitors decreased LPS-induced p38, MEK 1/2 and JNK phosphorylation, which may be explained by the cross-talk and feedback mechanisms between TLR4-mediated MAPK and the NF-κB signaling pathways (Figure 5B) (25–29). The inhibition of $cPLA_2$, 5-LOX, and sEH expressions following MAPK inhibition highlights the central role of MAPK signaling in shaping the oxylipin metabolome dynamics in septic mice.

We then investigated whether treatment with simvastatin or dLGG affects the phosphorylation and activation of MAPK proteins p38, MEK 1/2 and JNK and the expression levels of $cPLA_2$ and its downstream enzymes CYP450 (CYP4A), 5-LOX and sEH by Western blot analysis of liver protein homogenates from tested animals. Simvastatin treatment decreased LPS-induced activation or expression of MEK 1/2, $cPLA_2$ and CYP4A, whereas minimal or no effect on p38, JNK, 5-LOX and sEH expressions was observed (Figure 5C). In comparison, while dLGG treatment was observed to increase the ratio of p-JNK/JNK, dLGG pre- and posttreatment had more significant effects on inhibition of the signaling proteins and enzymes involved in oxylipin biosynthesis (p38, MEK 1/2, $cPLA_2$, 5-LOX, CYP4A, and sEH) than on those of simvastatin. These results are consistent with the observed oxylipin–metabolome profiles, wherein simvastatin or dLGG treatment attenuated LPS-induced overproduction of several proinflammatory oxylipin species derived from CYP450, 5-LOX and sEH activities, for example, HETEs, HODEs and EpOMEs. On the basis of the results in Figure 5, we conclude that the upstream events involved in the preventive effect of simvastatin on sepsis in mice was mainly through deregulation of MEK 1/2 signaling, while intervention of sepsis onset in mice by dLGG proceeded by deregulating the MEK 1/2 and p38 pathways. A proposed working model for the inhibitory effect of simvastatin and dLGG on endotoxin-induced activation of MAPK signaling and translocation of $cPLA_2$ is presented in Figure 6.

DISCUSSION

The roles of well-characterized cytokines in systemic inflammation are well understood; however, a better understanding of other inflammatory mediators including oxylipins is important for developing new and effective diagnostic tools and therapeutic regimens for sepsis (30). Metabolomics provides a powerful tool to map pathways implicated in varied pathology toward drug treatment. The results of the pathophysiological and comparative metabolomics approach used in this study illustrate a new direction for sepsis therapy, that is, the use of statins or plant galactolipid, dLGG. We demonstrated that simvastatin and dLGG are effective in shifting lipid mediator dynamics in sepsis partly by inducing production of endogenous proresolution and antiinflammatory oxylipin species. This is the first study to show that simvastatin affects oxylipin metabolite levels in the context of endotoxin shock, by increasing levels of antiinflammatory and proresolution LXA_4 both systemically and locally in the liver. The increase in 5(6)-EET levels compared with their downstream products, DHETs and THETs, suggests that simvastatin might have direct or indirect effects on sEH activities. We also demonstrated that dLGG is an enzyme inhibitor of 5-LOX and COX-2, and decreases the expression levels of CYP450, sEH and 5-LOX elevated by LPS in mouse liver. Simvastatin inhibits CYP450 and 5-LOX expressions to a lesser extent than dLGG. For both compounds, an increase in systemic 15-deoxy-PGJ_2 correlates with lower PPAR-γ expression in the lung tissues of all tested animals. This correlation suggests that initial PPAR-γ activation and consequent regulation might have several beneficial effects including greater neutrophil clearance in the early phases of sepsis progression (23). It is important to note, however, that this might not be the case for the later immunosuppressive state, wherein PPAR-γ induction is expected to be beneficial (30). We indeed observed that dLGG or simvastatin can elevate PPAR-γ levels in the lungs of septic mice induced by CLP. The attenuation of HIF-1α expressions in the kidneys by treatment with simvastatin or dLGG indicates the efficacy of both in ameliorating multiple organ damage. Renal damage is associated with inflammatory

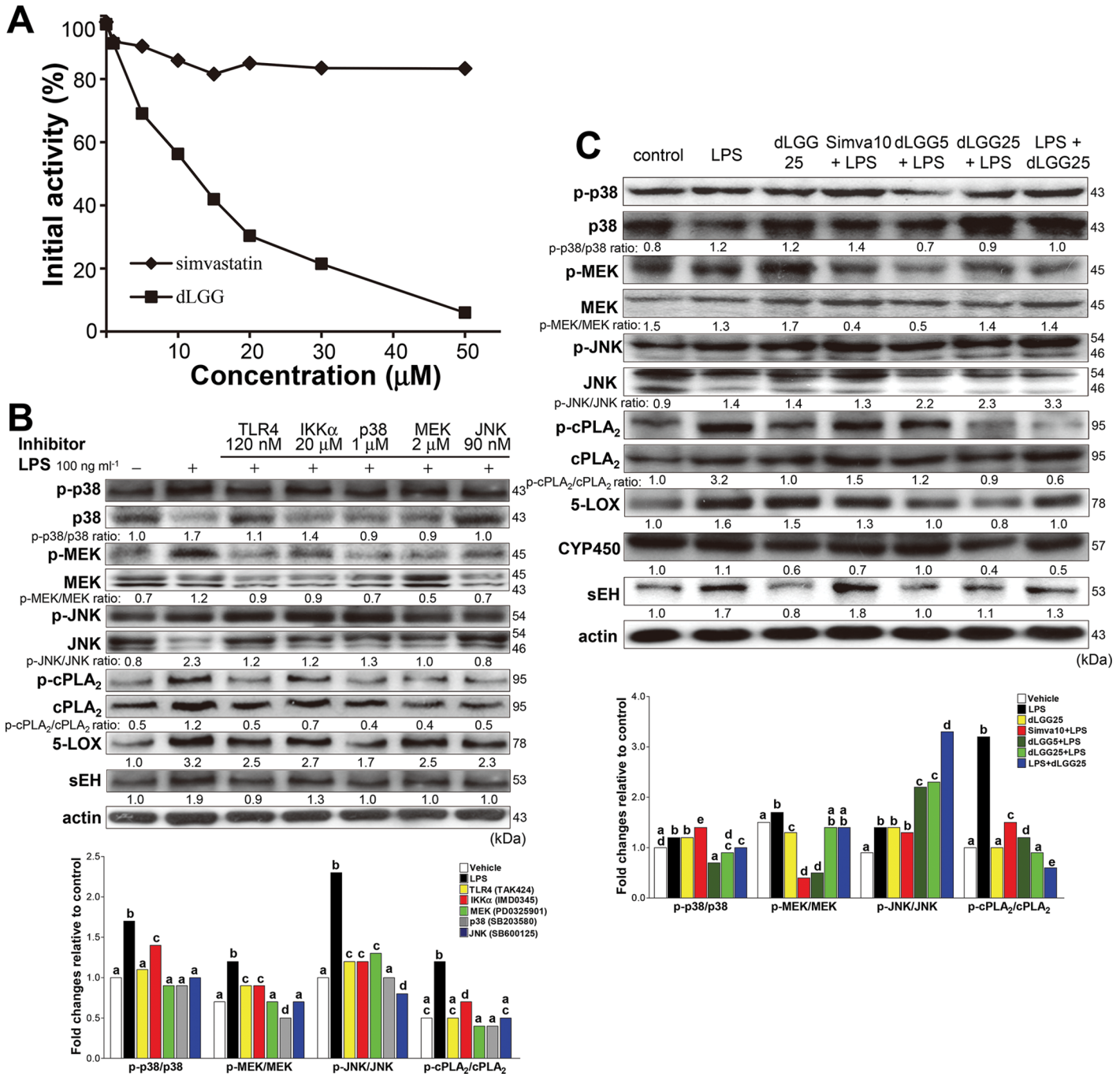

Figure 5. Effects of simvastatin and dLGG on activities and expression levels of lipid mediator-related proteins in the liver of septic mice and in LPS-stimulated macrophages. (A) The enzymatic activities of 5-LOX were determined in the presence of indicated concentrations of dLGG or simvastatin. (B) Western blot analyses of cellular proteins from LPS-stimulated RAW 264.7 macrophages treated with specific MAPK inhibitors or with dLGG at specific concentrations without causing cell toxicity. Representative blots are shown and densitometric analysis was used to quantify and compare results. (C) Western blot analyses for phospholipid release and oxidation-related proteins ($cPLA_2$, CYP450, sEH, 5-LOX) from liver homogenates from the different treatment groups. Representative blots are shown and densitometric analysis was used to quantify and compare results. Phosphorylation ratio of $cPLA_2$, p38 and MEK 1/2 to their original forms of protein among treatment groups in (B) and (C) are compared. Statistically significant fold-change increase or decrease compared with the protein expression levels of the vehicle control are marked by letters ($N = 4$, $P < 0.05$, ANOVA, *post hoc* LSD; values with different letters are significantly different).

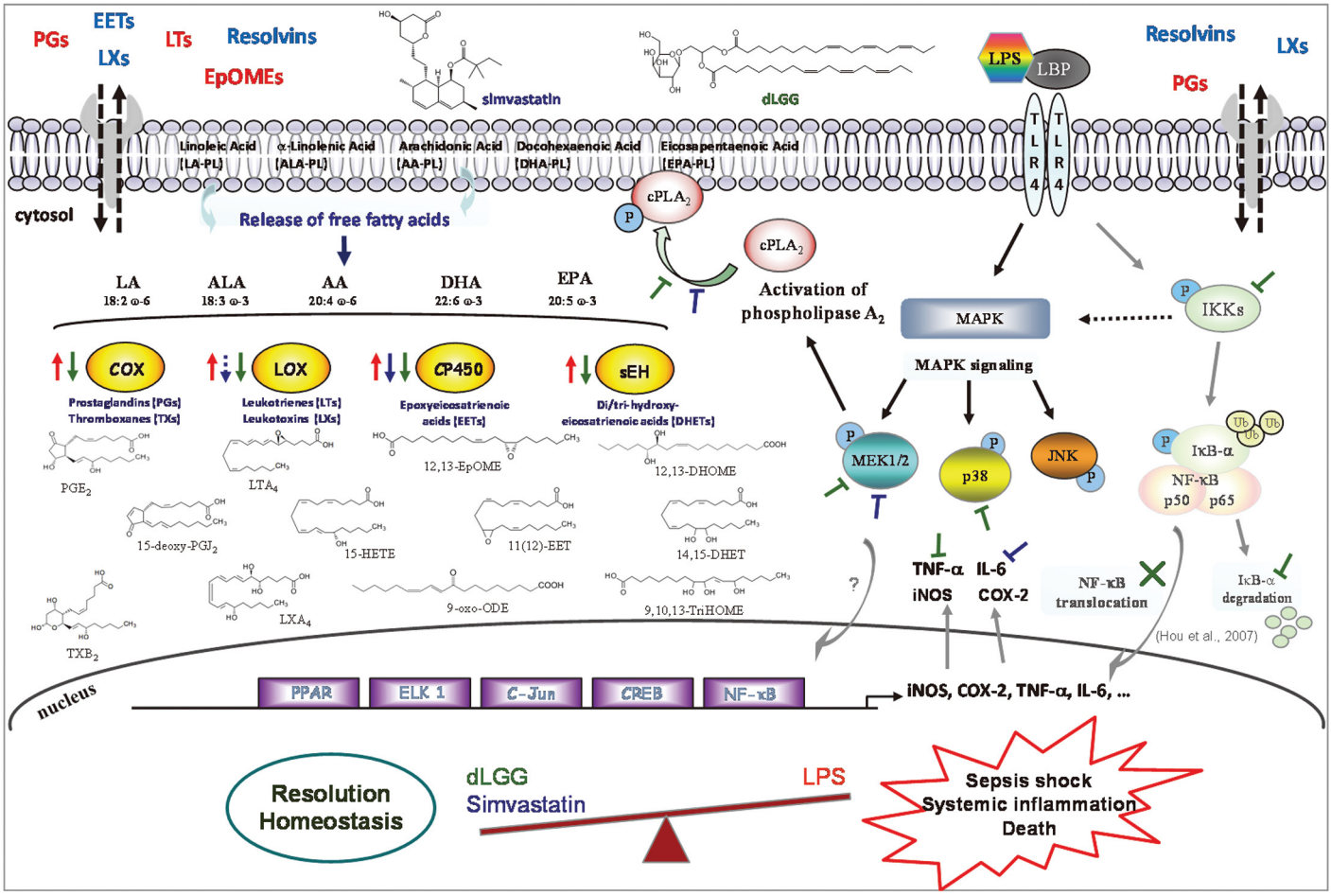

Figure 6. Simvastatin and dLGG mediate formation of oxylipin mediators by regulation of MAPK-induced cLPA$_2$ activation and downstream signaling cascades. Proposed working model for the inhibitory effect of simvastatin and dLGG on endotoxin-induced activation of MAPK signaling and translocation of cPLA$_2$. Free fatty acids are released and subsequently acted upon by various enzymes, LOX, COX, CYP450 and sEH. Balancing of intra- and extracellular cascade responses between proinflammation and antiinflammation are important in early sepsis, as it determines the fate of the organism either toward resolution and homeostasis or systemic inflammation and death.

cascades leading to the production of leukotoxins including HODEs and EpOMEs (31). Our results show that LPS treatment increased the systemic levels of these metabolites while levels after treatment with either simvastatin or dLGG were comparable to those of the vehicle control. These results suggest that simvastatin and dLGG protect against endotoxin-induced acute kidney injury (AKL) in animals.

In the serum, presence of higher levels of 9(10)- and 12(13)-EpOMEs and 9- and 13-oxo-ODE, LA epoxy and diol metabolites of CYP450, respectively, as well as of 9,10-13- and 9,12-13-TriHOMEs and their corresponding sEH metabolites in the LPS group, correlates well with the reported systemic toxicity attributed to these oxylipin species (32). These compounds were decreased by simvastatin or dLGG treatment. 8-, 12- and 15-HETE and TXB$_2$ were increased in the LPS group, with an apparent decrease in LXA$_4$. The reverse was observed for simvastatin and dLGG treatments where LXA$_4$ levels were increased. 8-, 12-, 15-HETE, and the downstream metabolites have systemic anti- and prothrombotic activities (33–35). They are also involved in pulmonary vascular smooth muscle remodeling and apoptosis (36–38), but complete understanding of the physiological roles of these metabolites remains unclear, especially in sepsis. LXA$_4$ has been extensively reported to have antiinflammatory and proresolution activities and has been associated with decreased systemic inflammation and reduced septic bacterial load (39). Other HETE species, for example, 20-HETE and 11-HETE, were not affected significantly by any of the treatments, but it seems likely that dLGG and simvastatin divert the fate of AA and LA oxidation, and shunt them toward production of antiinflammatory and proresolution species highlighted by the increase in 11(12)-EET for high-dose dLGG pretreatment and 5(6)-EET for simvastatin.

In the liver, levels of 9- and 13-HODE, 9,10- and 12,13-DiHOME, 9(10)- and 12(13)-EpOME, 9,12,13-TriHOME, 8-HETE, 19-HETE, 5-oxo-ETE, $PGE_{2,}$ and $PGF_{2\alpha}$ elevated in the LPS group were reversed by simvastatin and dLGG treatments. 19-HETE and prostanoids PGE_2 and $PGF_{2\alpha}$ are proinflammatory metabolites of AA; both prostanoids are produced from COX-2 and the subsequent action of specific inducible prostanoid synthases (40). Pretreatment with simvastatin or dLGG were characterized most significantly by the elevated levels of LXA_4 in the liver, while dLGG posttreatment can also increase EPA metabolites, resolvin D1 and 15-HEPE, and DHA and its metabolites, 17-HDoHE, 10,17-DiHDoHe. The increase in levels of DHA and corresponding substrates in the liver demonstrate the active production of pro- and antiinflammatory oxylipins needed for the maintenance of tissue homeostasis, while the apparent decrease in circulating oxylipins is most likely correlated to hyperinflammatory responses. The organ-specific and systemic decrease of epoxy and diol metabolites of LA from the LOX and sEH pathways following dLGG treatment indicate that dLGG can be used as a novel LOX or sEH inhibitor.

Several factors including intracellular calcium influx, p38, and MEK 1/2 phosphorylation have been reported to affect $cPLA_2$ activation in different cell types (41,42); however, the direct effects of the MAPK signaling cascade on the activation of downstream enzymes, specifically of 5-LOX, sEH, and CYP450, has not been reported. In this study, we demonstrate that the activation of $cPLA_2$ and its downstream enzymes resulting in free fatty acid oxidation is mediated by phosphorylation of MAPK proteins. Overproduction of LPS-induced inflammatory oxylipins derived from these pathways could be attenuated by treatment with either simvastatin or dLGG through the inhibition of MEK 1/2 and/or p38 activation that may lead to restoration of homeostasis in septic animals.

CONCLUSION

This report to reveal that simvastatin and dLGG can inhibit MEK phosphorylation *in vivo* and regulate endogenous metabolite levels in the liver and in circulation. Efficacy of either compound in the LPS-induced endotoxemia and CLP-induced sepsis models show their potential in prevention and intervention. Using targeted oxylipin profiling as a tool for phenotyping the septic and homeostatic signature, we demonstrate that both simvastatin and dLGG warrant further development as novel therapeutic agents for sepsis as highlighted by their efficacy in altering oxylipin profiles and increasing the ratios of proresolution oxylipins in a murine models of sepsis.

ACKNOWLEDGMENTS

We thank Bing-Ying Ho for technical assistance, Miranda Loney for English editorial assistance, and the Metabolomics Core Facility and Laboratory Animal Core Facility of the Agricultural Biotechnology Research Center, Academia Sinica, Taiwan. This study was supported by grant funding from the Ministry of Science and Technology (NSC 100-2321-B-400-002 and NSC-102-2325-B-001-007) and institutional grant funding from Academia Sinica, Taiwan.

DISCLOSURE

The authors declare that they have no competing interests as defined by *Molecular Medicine*, or other interests that might be perceived to influence the results and discussion reported in this paper.

REFERENCES

1. Lever A, Mackenzie I. (2007). Sepsis: definition, epidemiology, and diagnosis. *BMJ*. 335:879–883.
2. Dellinger RP, *et al*. (2008). Surviving Sepsis Campaign: international guidelines for management of severe sepsis and septic shock. *Intensive Care Med*. 39:165–228.
3. Jawad I, Luksic I, Rafnsson SB. (2012). Assessing available information on the burden of sepsis: global estimates of incidence, prevalence and mortality. *J. Glob. Health*. 2:010404.
4. Fullerton JN, O'Brien AJ, Gilroy DW. (2014). Lipid mediators in immune dysfunction after severe inflammation. *Trends Immunol*. 35:12–21.
5. Serhan CN, *et al*. (2000). Novel functional sets of lipid-derived mediators with antiinflammatory actions generated from omega-3 fatty acids via cyclooxygenase 2-nonsteroidal antiinflammatory drugs and transcellular processing. *J. Exp. Med*. 192:1197–204.
6. Yang J, Schmelzer K, Georgi K, Hammock BD. (2009). Quantitative profiling method for oxylipin metabolome by liquid chromatography electrospray ionization tandem mass spectrometry. *Anal. Chem*. 81:8085–93.
7. Bannenberg GL. (2010). Therapeutic applicability of anti-inflammatory and proresolving polyunsaturated fatty acid-derived lipid mediators. *ScientificWorldJournal*. 10:676–712.
8. Aikawa M, Libby P. (2004). Lipid lowering therapy in atherosclerosis. *Semin. Vasc. Med*. 4:357–66.
9. Merx MW, *et al*. (2005). Statin treatment after onset of sepsis in a murine model improves survival. *Circulation*. 112:117–24.
10. Almuti K, Rimawi R, Spevack D, Ostfeld RJ. (2006). Effects of statins beyond lipid lowering: potential for clinical benefits. *Int. J. Cardiol*. 109:7–15.
11. Birnbaum Y, Ye Y. (2012). Pleiotropic Effects of Statins: The Role of Eicosanoid Production. *Curr. Atheroscler. Rep*. 14:135–9.
12. Almog Y, *et al*. (2004). Prior statin therapy is associated with a decreased rate of severe sepsis. *Circulation*. 110:880–5.
13. Novack V, *et al*. (2009). The effects of statin therapy on inflammatory cytokines in patients with bacterial infections: a randomized double-blind placebo controlled clinical trial. *Intensive Care Med*. 35:1255–60.
14. Yang TF, *et al*. (2014). Effect of statin therapy on mortality in patients with infective endocarditis. *Am. J. Cardiol*. 114:94–9.
15. Calder PC. (2006). n-3 polyunsaturated fatty acids, inflammation, and inflammatory diseases. *Am. J. Clin. Nutr*. 83(6 Suppl):1505S–19S.
16. Williams CM, Burdge G. (2006). Long-chain n-3 PUFA: plant v. marine sources. *Proc. Nutr. Soc*. 65:42–50.
17. Hou CC, *et al*. (2007). A galactolipid possesses novel cancer chemopreventive effects by suppressing inflammatory mediators and mouse B16 melanoma. *Cancer Res*. 67:6907–15.
18. Limdi JK, Hyde GM. (2003). Evaluation of abnormal liver function tests. *Postgrad. Med. J*. 79:307–12.
19. Rittirsch D, Huber-Lang MS, Flierl MA, Ward PA. (2009). Immunodesign of experimental sepsis by cecal ligation and puncture. *Nat. Protoc*. 4:31–6.
20. Gustot T. (2011). Multiple organ failure in sepsis: prognosis and role of systemic inflammatory response. *Curr. Opin. Crit. Care*. 17:153–9.
21. Yasuda H, Yuen PS, Hu X, Zhou H, Star RA. (2006). Simvastatin improves sepsis-induced mortality and acute kidney injury via renal vascular effects. *Kidney Int*. 69:1535–42.

22. Ejima K, *et al*. (2003). Cyclooxygenase-2-deficient mice are resistant to endotoxin-induced inflammation and death. *FASEB J*. 17:1325–7.
23. Reddy RC, Narala VR, Keshamouni VG, Milam JE, Newstead MW, Standiford TJ. (2008). Sepsis-induced inhibition of neutrophil chemotaxis is mediated by activation of peroxisome proliferator-activated receptor-γ. *Blood*. 112:4250–8.
24. Standiford TJ, Keshamouni VG, Reddy RC. (2005). Peroxisome proliferator-activated receptor-γ as a regulator of lung inflammation and repair. *Proc. Am. Thorac. Soc*. 2:226–31.
25. Yuan ZQ, *et al*. (2002). Inhibition of JNK by cellular stress- and tumor necrosis factor alpha-induced AKT2 through activation of the NF-κB pathway in human epithelial cells. *J. Biol. Chem*. 277:29973–82.
26. Dajani R, *et al*. (2007). Pleiotropic functions of TNF-α determine distinct IKKβ-dependent hepatocellular fates in response to LPS. *Am. J. Physiol. Gastrointest Liver Physiol*. 292:G242–52.
27. Arthur JSC, Ley SC. (2013). Mitogen-activated protein kinases in innate immunity. *Nat. Rev. Immunol*. 13:679–92.
28. Slomiany BL, Slomiany A. (2013). Induction in gastric mucosal prostaglandin and nitric oxide by Helicobacter pylori is dependent on MAPK/ERK-mediated activation of IKKβ and $cPLA_2$: modulatory effect of ghrelin. *Inflammopharmacol*. 21:241–51.
29. Bruegel M, *et al*. (2012). Sepsis-associated changes of the arachidonic acid metabolism and their diagnostic potential in septic patients. *Crit. Care Med*. 40:1478–86.
30. Zingarelli B, Sheehan M, Hake PW, O'Connor M, Denenberg A, Cook JA. (2003). Peroxisome proliferator activator receptor-γ ligands, 15-deoxy-δ(12,14)-prostaglandin J2 and ciglitazone, reduce systemic inflammation in polymicrobial sepsis by modulation of signal transduction pathways. *J. Immunol*. 171:6827–37.
31. Crouser ED, *et al*. (2004). Abnormal permeability of inner and outer mitochondrial membranes contributes independently to mitochondrial dysfunction in the liver during acute endotoxemia. *Crit. Care Med*. 32(2):478–88.
32. Nie X, Song S, Zhang L, Qiu Z, Shi S, Liu Y. (2012). 15-Hydroxyeicosatetraenoic acid (15-HETE) protects pulmonary artery smooth muscle cells from apoptosis via inducible nitric oxide synthase (iNOS) pathway. *Prostaglandins Other Lipid Mediat*. 97:50–9.
33. Sordi R, Menezes-de-Lima O Jr, Horewicz V, Scheschowitsch K, Santos LF, Assreuy J. (2013). Dual role of lipoxin A4 in pneumosepsis pathogenesis. *Int. Immunopharmacol*. 17:283–92.
34. Porro B, Songia P, Squellerio I, Tremoli E, Cavalca V. (2014). Analysis, physiological and clinical significance of 12-HETE: a neglected platelet-derived 12-lipoxygenase product. *J Chromatogr. B Analyt. Technol. Biomed. Life Sci*. 964:26–40.
35. Askari AA, Thomson S, Edin ML, Lih FB, Zeldin DC, Bishop-Bailey D. (2014). Basal and inducible anti-inflammatory epoxygenase activity in endothelial cells. *Biochem. Biophys. Res. Commun*. 446:633–7.
36. Tunctan B, *et al*. (2012). A novel treatment strategy for sepsis and septic shock based on the interactions between prostanoids, nitric oxide, and 20-hydroxyeicosatetraenoic acid. *Antiinflamm. Antiallergy Agents Med. Chem*. 11:121–50.
37. Serhan CN, Clish CB, Brannon J, Colgan SP, Gronert K, Chiang N. (2000). Anti-microinflammatory lipid signals generated from dietary N-3 fatty acids via cyclooxygenase-2 and transcellular processing: a novel mechanism for NSAID and N-3 PUFA therapeutic actions. *J. Physiol. Pharmacol*. 51(4 Pt 1):643–54.
38. Gladine C, *et al*. (2014). Lipid profiling following intake of the omega 3 fatty acid DHA identifies the peroxidized metabolites F4-neuroprostanes as the best predictors of atherosclerosis prevention. *PLoS One*. 9:e89393.
39. Walker J, *et al*. (2011). Lipoxin A4 increases survival by decreasing systemic inflammation and bacterial load in sepsis. *Shock*. 36:410–6.
40. Qi HY, Shelhamer JH. (2005). Toll-like receptor 4 signalling regulates cytosolic phospholipase A2 activation and lipid generation in lipopolysaccharide-stimulated macrophages. *J Biol. Chem*. 280:38969–75.
41. Chakraborti S, *et al*. (2012). Role of PKCα-p(38) MAPK-G(i)α axis in NADPH oxidase derived O(2)(.-)-mediated activation of cPLA(2) under U46619 stimulation in pulmonary artery smooth muscle cells. *Arch. Biochem. Biophys*. 523:169–180.
42. Kuan YH, Huang FM, Lee SS, Li YC, Chang YC. (2013). Bisgma stimulates prostaglandin E2 production in macrophages via cyclooxygenase-2, cytosolic phospholipase A2, and mitogen-activated protein kinases family. *PLoS One*. 8:e82942

Cite this article as: Apaya MK, *et al*. (2015) Simvastatin and a plant galactolipid protect animals from septic shock by regulating oxylipin mediator dynamics through the MAPK-$cPLA_2$ signaling pathway. *Mol. Med*. 21:988–1001.